

## **Effect of fiber length on direct tensile and impact strength of cement-based composites containing silica fume**

An Cheng<sup>1)</sup>, \*Wei-Ting Lin<sup>2)</sup>, Hui-Mi Hsu<sup>3)</sup>, Sao-Jeng Chao<sup>4)</sup>, Wei-Yuan Dai<sup>5)</sup> and Chih-Cheng Huang<sup>6)</sup>

1), 2), 3), 4), 5) *Department of Civil Engineering, National Ilan University, Ilan 260, Taiwan*

2), 6) *Institute of Nuclear Energy Research, Atomic Energy Council, Executive Yuan, Taoyuan 325, Taiwan*

<sup>2)</sup> *wtlin@niu.edu.tw*

### **ABSTRACT**

This study is aimed to evaluate the tensile strength and impact resistance of cement-based composites which comprise steel fibers and silica fume in the mixes. Material variables include water-binder ratio, dosage of silica fume, steel fiber length and dosage. A designed tensile strength was used to perform the direct tensile in this study. Test results indicate that the compressive strength, splitting tensile strength and direct tensile strength of specimens for fiber length of 60 mm are higher than that of 35 mm. The inclusion of fibers in specimens containing silica fume has higher compressive and tensile strength; and lower impact resistance than the specimens made with silica fume. Incorporation of steel fiber and silica fume in composites achieves significantly higher increase in compressive strength, splitting tensile strength, and direct tensile strength than only individual use of steel fiber or silica fume and decrease in impact resistance than only individual use of steel fiber. In addition, the compressive strength, splitting tensile strength, direct tensile strength and impact resistance are fairly correlated by regression analysis. Finally, the proposed direct tensile testing method is suitable for determining the tensile strength of fiber reinforce cement-based composites and generating the tensile stress-strain curves easily.

**Keywords:** direct tensile strength, impact resistance, fiber length, stress-strain curves

---

<sup>1)</sup> Associate Professor

<sup>2)</sup> Assistant Professor and Associate Engineer

<sup>3)</sup> Professor

<sup>4)</sup> Professor

<sup>5)</sup> Graduate student

<sup>6)</sup> Research Fellow

## 1. INTRODUCTION

In general, the constituents of cement-based composites include cementitious material, water, aggregate and/or additives. Fiber is one of the commercially available additives and has been added in cement-based composites since 1960 to enhance composite properties, particularly tensile strength, abrasion resistance and energy absorbing capacity (Chalioris 2009; Kang 2011; Sahin 2011). The presence of fiber refrains the growth or propagation of internal cracks and helps to transfer load (Lee 2012). The composites with fiber have much higher ductility than those without fiber, and demonstrate a significant increase in energy absorption or toughness (Kesner 2005). Therefore, fiber reinforced cement-based composites is used worldwide in high-rises, large span bridges, highways, and airport runways over past decades.

Supplementary cementitious materials such as silica fume, fly ash, and ground granulated blast-furnace slag (ggbfs), are able to as by-product recycled materials contributed to the properties of cement-based composites through either pozzolanic activity or hydration reaction (Lothenbach 2011). Silica fume has a larger specific surface area, finer particle and higher  $\text{SiO}_2$  content compared to those of fly ash and ggbfs. Hence, the pozzolanic reaction rate of silica fume is considerably higher than that of fly ash or ggbfs. The high amorphous silica content can densify the microstructure and improves strength, permeability, and other properties (Lin 2011). The use of silica fume is also beneficial to increase in the interfacial bond between paste and aggregates. For the fiber reinforced cement-based composites, it is also reported that the combination of silica fume with steel fiber can effectively enhance the compressive strength, splitting tensile strength, abrasion resistance and impact resistance and is beneficial to fiber dispersion in cement-based composites (Nili 2012; Chung 2002). Silica fume also increases the bonding between fiber and mortar (Nili 2012; Chung 2002).

On the other hand, the compressive strength and tensile strength are the principal properties employed in the design of reinforced and prestressed concrete structures. For the tensile strength, unlike metals it is difficult to obtain direct tensile strength of concrete due to the brittleness. No standard test method has been adopted by ASTM to provide a direct measurement of tensile strength of concrete. Indirect methods included in ASTM are standard test method for splitting tensile strength of cylindrical concrete specimens in accordance with ASTM C496 and for flexural strength of concrete with ASTM C78. In addition, a proper direct tensile testing method can be used to estimate the tensile strength of composites. A direct test result provides a uniaxial and approximately real tensile strength of cement-based composites.

Many previous researchers have studied either steel fibers or ultrafine silica fume individually; however, few studies have evaluated the combination of steel fibers and ultrafine silica fume mixed into concrete. This study is aimed to evaluate the strength and impact behavior of cement-based composites using steel fiber and silica fume. Silica fumes are tested to demonstrate the ability to enhance the microstructure of the cement-based composites while steel fibers are tested to demonstrate the ability to inhibit crack initiation and reduce crack propagation. Three fiber dosages (0 %, 0.5 % and 1.0 % by volume of composites), two silica fume contents (0 % and 5 % by weight of cement), two fiber lengths (35 mm and 60 mm) and two water-binder ratios (0.35 and

0.55) were used in the mix design. Strength of cement-based composites was evaluated using compressive strength, splitting strength, direct tensile strength and impact resistance as measures.

## 2. EXPERIMENTAL PROGRAM

### 2.1 Materials and Mix Proportion

In this study, type I Portland cement conforming to ASTM C150 was used in all mixes. Silica fume with a specific gravity of 2.20 and surface area of 22500 m<sup>2</sup>/kg was used and the amount of SiO<sub>2</sub> in silica fume was 91.5 %. The diameter of silica fume particle was about 0.1-0.2 μm. Silica fume (0 % and 5 % by weight of cement) was added to partially replace cement.

Steel fiber used was hooked-end fiber with an aspect ratio ( $l/d$ ) of 65. The average length of steel fiber was 35 mm and 60 mm, and tensile strength of steel fiber was 1100 N/mm<sup>2</sup>. Three volume fractions ( $V_f=0, 0.5$  and 1.0 %) were selected for each mix.

The maximum size of coarse aggregate was 13 mm and the fineness modulus of fine aggregate was 2.87. The water-binder ratio (w/b) of 0.35 and 0.55 were selected and the mix proportions for concrete specimens are given in Table 1. The coding used to identify "Mix No." in column one of Table 1 should read: "A" and "B", to represent the w/b of 0.35 and 0.55; "5", to represent the dosages of silica fume at 5 %; "S" and "L", to represent the short and long steel fiber; and "1" and "2", to represent the volume fractions of steel fiber at 0.5 % and 1.0 %. Mixture slump was around 150 mm by using a high-range water-reducing admixture.

Table 1 Mix design (kg/m<sup>3</sup>)

| Mix no. | w/b  | Water | Cement | Silica fume | FG*   | CG**  | Fiber | SP*** |
|---------|------|-------|--------|-------------|-------|-------|-------|-------|
| A       | 0.35 | 189.4 | 558.0  | 0           | 908.0 | 700.0 | 0     | 5.6   |
| A01S    | 0.35 | 189.4 | 558.0  | 0           | 901.0 | 694.0 | 39.0  | 5.6   |
| A02S    | 0.35 | 189.4 | 558.0  | 0           | 894.0 | 687.0 | 78.0  | 5.6   |
| A01L    | 0.35 | 189.4 | 558.0  | 0           | 901.0 | 694.0 | 39.0  | 5.6   |
| A02L    | 0.35 | 189.4 | 558.0  | 0           | 894.0 | 687.0 | 78.0  | 5.6   |
| A5      | 0.35 | 189.4 | 530.1  | 27.9        | 908.0 | 700.0 | 0     | 5.6   |
| A51S    | 0.35 | 189.4 | 530.1  | 27.9        | 901.0 | 694.0 | 39.0  | 5.6   |
| A52S    | 0.35 | 189.4 | 530.1  | 27.9        | 894.0 | 687.0 | 78.0  | 5.6   |
| A51L    | 0.35 | 189.4 | 530.1  | 27.9        | 901.0 | 694.0 | 39.0  | 5.6   |
| A52L    | 0.35 | 189.4 | 530.1  | 27.9        | 894.0 | 687.0 | 78.0  | 5.6   |
| B       | 0.55 | 217.0 | 395.0  | 0           | 908.0 | 780.0 | 0     | 0     |
| B01S    | 0.55 | 217.0 | 395.0  | 0           | 901.0 | 773.0 | 39.0  | 0     |
| B02S    | 0.55 | 217.0 | 395.0  | 0           | 894.0 | 767.0 | 78.0  | 0     |
| B01L    | 0.55 | 217.0 | 395.0  | 0           | 901.0 | 773.0 | 39.0  | 0     |
| B02L    | 0.55 | 217.0 | 395.0  | 0           | 894.0 | 767.0 | 78.0  | 0     |
| B5      | 0.55 | 217.0 | 375.2  | 19.8        | 908.0 | 780.0 | 0     | 0     |
| B51S    | 0.55 | 217.0 | 375.2  | 19.8        | 901.0 | 773.0 | 39.0  | 0     |
| B52S    | 0.55 | 217.0 | 375.2  | 19.8        | 894.0 | 767.0 | 78.0  | 0     |
| B51L    | 0.55 | 217.0 | 375.2  | 19.8        | 901.0 | 773.0 | 39.0  | 0     |
| B52L    | 0.55 | 217.0 | 355.5  | 19.8        | 894.0 | 767.0 | 78.0  | 0     |

\*fine aggregate \*\*coarse aggregate \*\*\*superplasticizer

## 2.2 Specimens

Specimens of 20 different mixes were cast. For each mix, twenty-one  $\psi 100 \times 200$  mm cylindrical specimens for compressive and splitting strength test were used. Three  $\psi 150 \times 300$  mm and three  $\psi 150 \times 50$  mm cylindrical specimens were used for the direct tensile strength test and impact test, respectively. All the specimens were cured in saturated lime-water until testing.

## 2.3 Test Methods

The compressive strength test at ages of 7, 14, 28, 56, 91 and 150 days were performed in accordance with ASTM C39. The splitting tensile strength test at the age of 150 days was conducted in accordance with ASTM C496.

The designed direct tensile testing method is a relatively new test that is a modified version of those in previous studies (Swaddiwudhipong 2003; Lee 2012) as shown in Fig. 1. Two lengths of rebar (#6) were placed along the longitudinal axis of the  $\psi 150 \times 300$  cylindrical specimen. A 10 mm diameter hole was drilled to a depth of 25 mm in the center of one rebar; the other rebar was machined into a  $\psi 10$  mm cylindrical plug at one end. To test the tensile strength, the exposed sections of the rebar were subjected to a load of 50 kgf/min until failure. With the exception of compressive strength tests, all specimens were maintained in a curing room until the age of 150 days prior to testing.

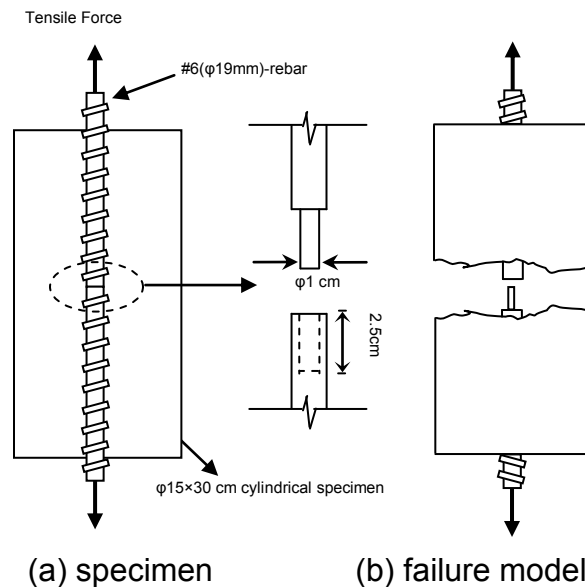


Fig. 1 Schematic description of direct tensile testing

The impact resistance was performed at the age of 150 days following the recommendation of ACI committee 544. It is suggested to repeat to drop a 63.5 mm-diameter and 4.54 kg steel ball from a height of 914 mm on the specimen until the first visible crack is found and then to record the drop number. Failure is defined as the crack opening to let specimen touch at least three of the four positioning lugs on the base plate.

### 3. RESULTS AND DISCUSSION

#### 3.1 Compressive Strength

The compressive strength curves of A, A5, B and B5 specimens are plotted in Fig. 2. From those results, the compressive strength at the age of 90 days is little different from the strength at age of 56 days for mix B groups and the 150 days strength is about the same as 91 days strength for each mixes. At the age of 150 days, the inclusion of silica fume increases compressive strength around 5 %, which results from pozzolanic reaction.

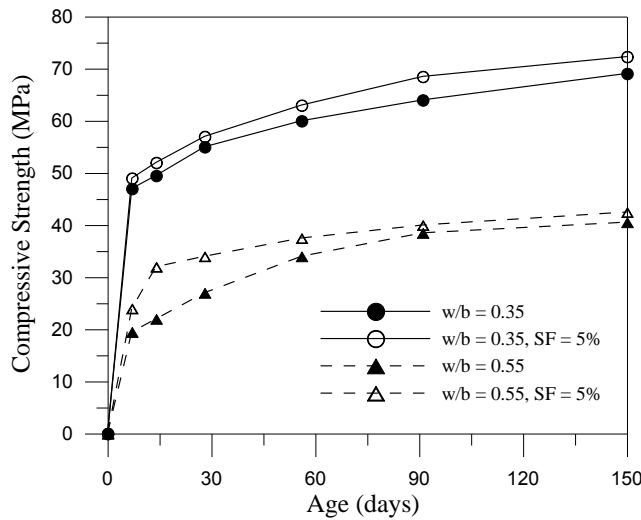


Fig. 2 Compressive strength development curves

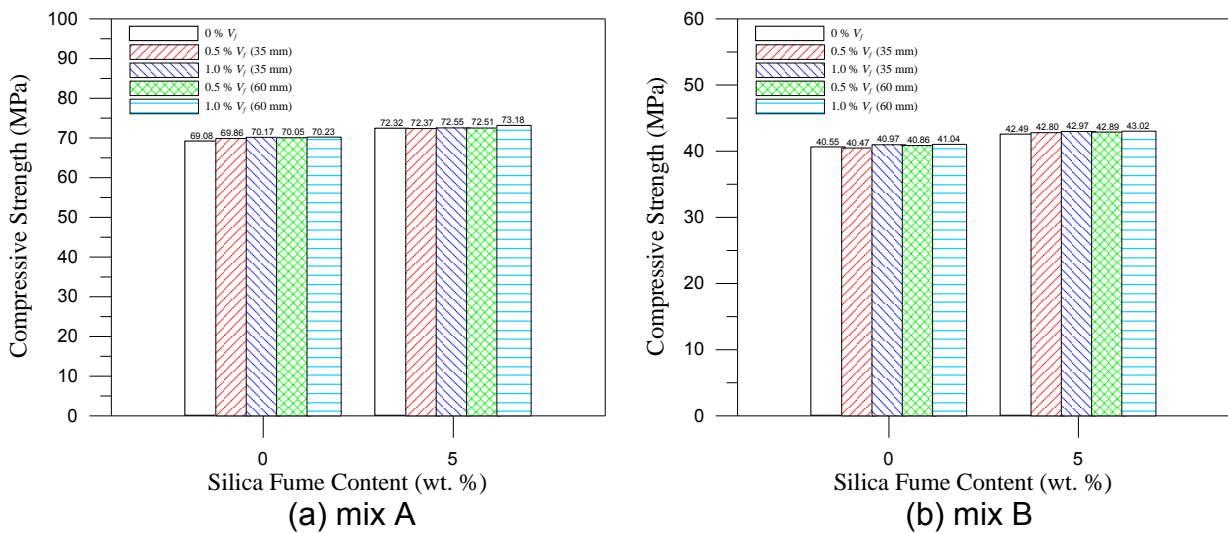


Fig. 3 Compressive strength histograms

The compressive strength histograms of specimens containing silica fume and steel fibers at the age of 150 days are illustrated in Figs. 3(a) and 3(b), respectively. The compressive strength increases with the silica fume, steel fiber and fiber length increases. The addition of fiber has less effect on the compressive strength by comparing with silica fume application. However, the compressive strength of specimens for fiber length of 60 mm is higher than that of 35 mm and the intension is up to 1 %-3 %. The fiber bridging can inhibit crack formation under axial loading. For a given w/cm ratio, specimen with 5% silica fume and 1% length fiber (60 mm) has highest compressive strength.

### 3.2 Splitting Strength

The splitting strength histograms of specimens containing silica fume and steel fibers at the age of 150 days are illustrated in Figs. 4(a) and 4(b), respectively. The splitting strength increases with the silica fume, steel fiber and fiber length increases. The addition of fiber has significantly effect on the compressive strength by comparing with silica fume application, especially for long length fiber. For the lower w/b ratio, the B01S, B01L, B02S and B02L specimens increase the splitting strength by 20.3 %, 22.6 %, 27.9 % and 32.8 %, respectively. The A01S, A01L, A02S and A02L specimens exhibit a larger increase of approximately 12.4 %, 22.5 %, 34.9 % and 39.2 % in the splitting strength, respectively. The crack stitching and multiple cracking effects of steel fibers are likely to help increase tensile resistance when the concrete specimens are cracked. Hence, the incorporation of fibers into cement-based composites is considered as an effective way to reduce cracking.

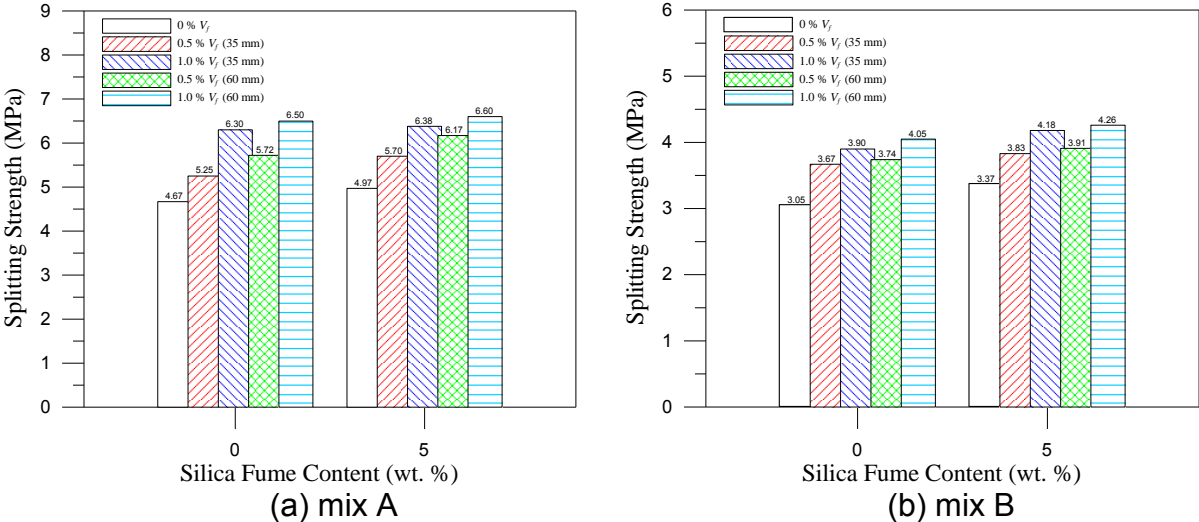


Fig. 4 Splitting strength histograms

The addition of silica fume in steel fiber cement-based composites plays an important role in splitting tensile strength by considerably increasing resistivity to cracking and the bonding between fiber and paste. The intension of splitting strength for mix A and B is about 3 % to 10 %. The maximum increasing percentage of the splitting strength is about 41.3 % and 39.7 % by incorporating 5 % silica fume and 1.0

% long fiber for the w/b ratio of 0.35 and 0.55, respectively. The fibers increase the ability of crack arresting greatly and delay in microcracks' propagation to macroscopic level. The presence of fiber also refrains the growth or propagation of internal cracks and helps to transfer load.

### 3.3 Direct Tensile Strength

The direct tensile strength histograms of specimens containing silica fume and steel fibers at the age of 150 days are shown in Figs. 5(a) and 5(b), respectively. The results show that the addition of silica fume or steel fiber obviously increases the direct tensile strength and the increasing trend is similar to the splitting strength. In addition, the specimens combining ultrafine silica fumes with steel fibers demonstrated superior performance to the specimens containing individual constituents of silica fume or fibers.

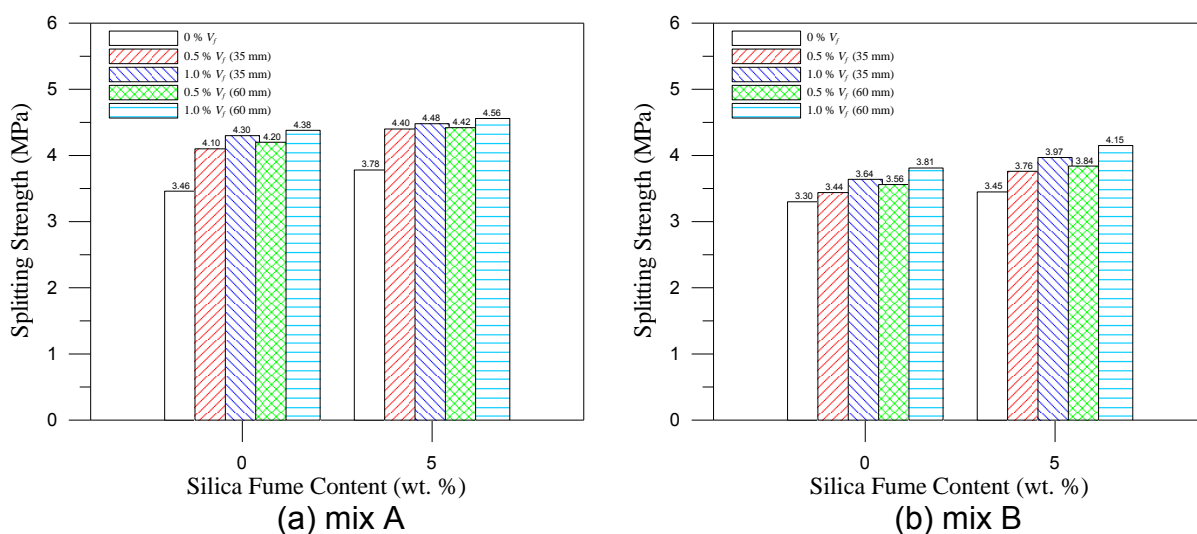


Fig. 5 Direct tensile strength histograms

The direct tensile strength test could generate the stress-strain curve and those curves represent the strain capacity and toughness. The tensile stress-strain curves of the specimens with short and long steel fibers at the w/b ratio of 0.35 are shown in Figs. 6(a) and 6(b), respectively. The strain capacity and toughness increase as the inclusion of fiber increases. It also represents the higher elastic modulus under axial tension.

Comparison of the difference between splitting and direct tensile strength, the splitting strengths are higher than the direct tensile strengths for all the specimens, but exceeded the B and B5 specimens at the higher w/b ratio. For the lower w/b ratio, the splitting strength of those specimens is 28 % to 48 % higher than the direct tensile strength. But at the higher w/b ratio, it is only about 2 % to 7 % higher than the direct tensile strength. This may be the result that silica fume also improves the bond between fiber and matrix because of the extra dense C-S-H gel obtained by its addition, particularly at a lower w/b ratio. Combination of silica fumes and steel fibers in the composites at the lower w/b ratio would more effectively increase the tensile properties. And the direct tensile testing method is suitable for determining the tensile strength of cement-based composites. By regression, good correlations are found between the

compressive strength and the splitting strength or direct tensile strength (full lines represent splitting strength and dotted line represent direct tensile strength) as shown in

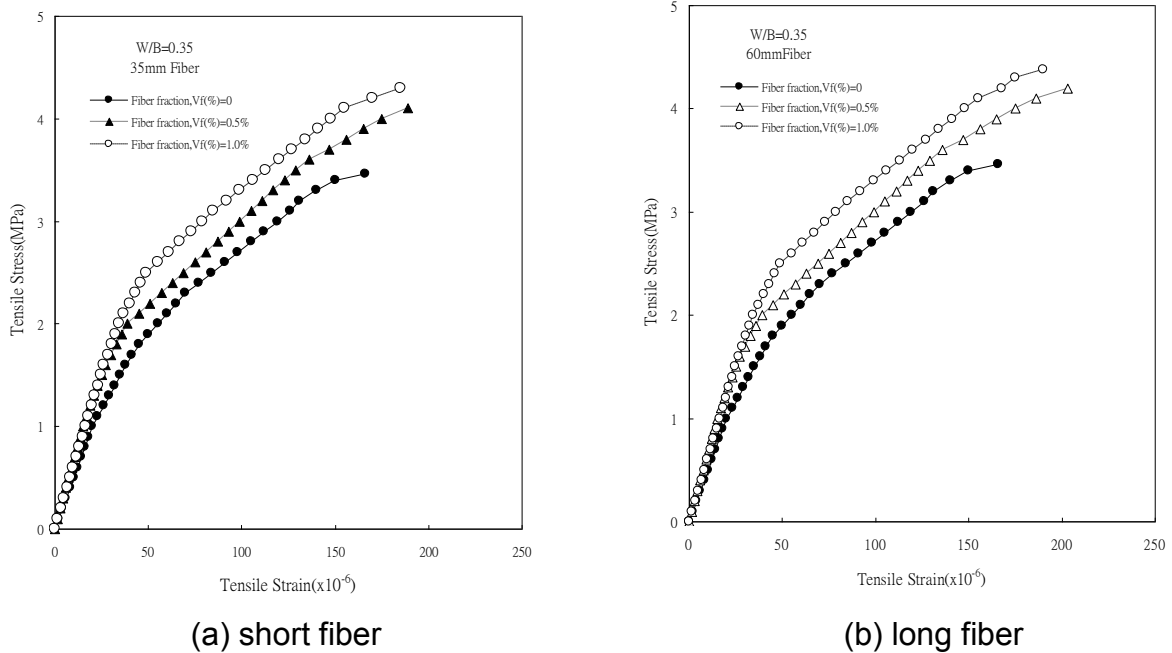


Fig. 6 Direct tensile strength histograms

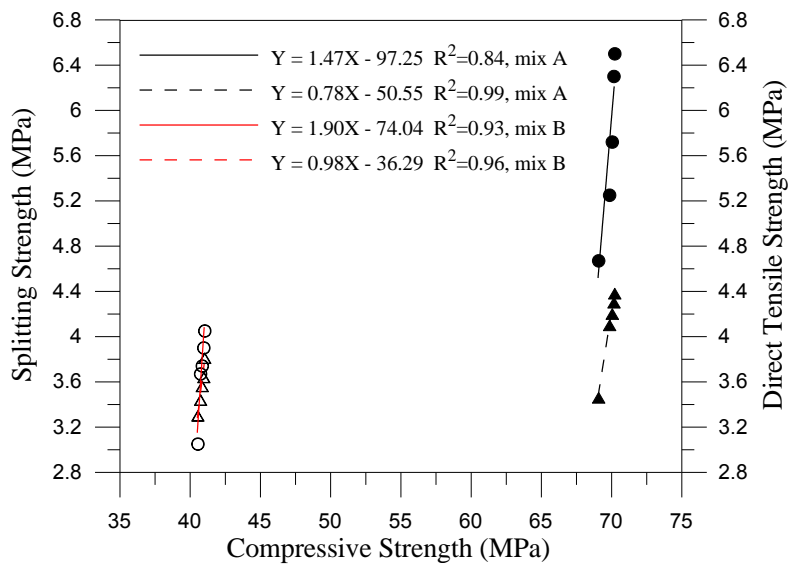


Fig. 7 Relationship between compressive and tensile

### 3.4 Impact Resistance

In accordance with ACI committee 544, the difference between N1 (impact number of initial crack) and N2 (impact number of failure) can be used as a qualitatively index of

impact resistance for cement-based composites. The impact resistance histograms of specimens containing silica fume and steel fibers at the age of 150 days are shown in Figs. 8(a) and 8(b), respectively. As the incorporation of steel fiber and silica fume increases the strength increases, and also increase the impact resistance. Steel fibers in the composites can restrain the extension of the crack, change the direction of crack growth and delay the growth rate of the crack, and silica fume can improve the interfacial characteristics. Thus, a combination of 6 % silica fume and 1.0 % long fibers at the lower w/b ratio provided the best impact performance. In addition, the impact resistance appears to increase linearly with compressive strength and direct tensile strength (full lines represent direct tensile strength and dotted line represent impact resistance) as illustrated in Fig. 9.

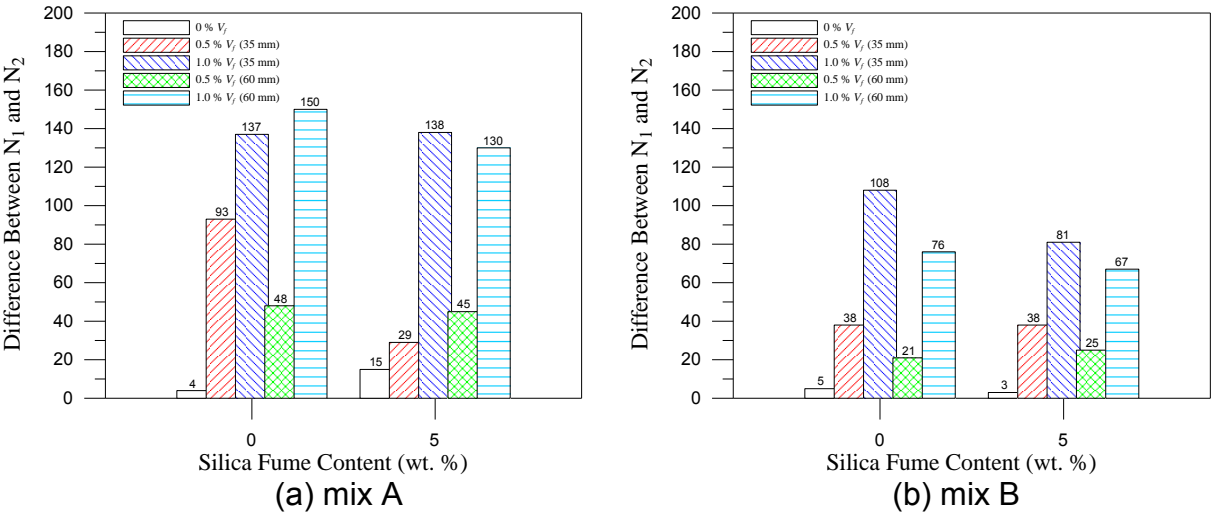


Fig. 8 Impact resistance histograms

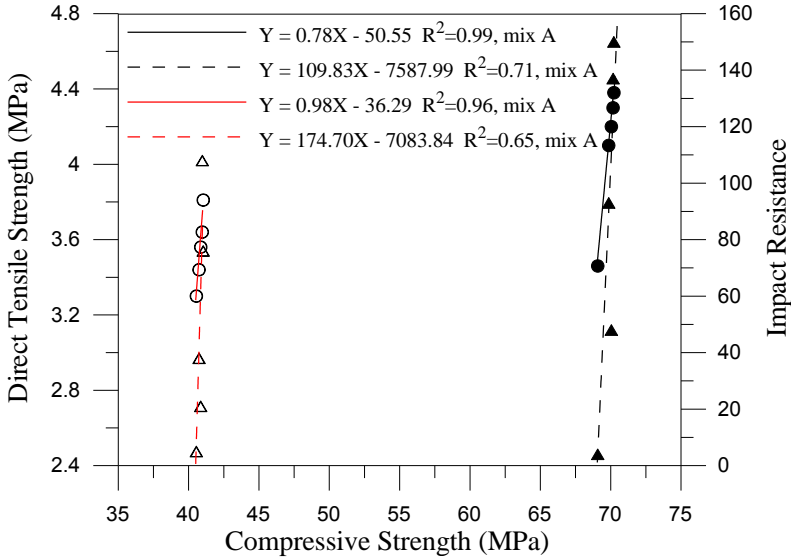


Fig. 9 Relationship between strength and impact test

## 4. CONCLUSIONS

The inclusion of silica fume and steel fibers demonstrates better strength and impact performance than the specimens containing individual constituents of silica fume or fibers. The performance of the specimens containing long fibers is greater than those specimens containing short fibers. Besides, the designed direct tensile testing method is suitable for determining the tensile strength of cement-based composites and generates the tensile stress-strain curves easily. Based on the regression analysis, the tensile strength and impact resistance can be reasonably corrected with the compressive strength.

## REFERENCES

- Chalioris, C.E. and Karayannis, C.G. (2009), "Effectiveness of the use of steel fibres on the torsional behavior of flanged concrete beams," *Cem. Concr. Compos.*, **31**(5), 331-341.
- Chung, D.D.L. (2002), "Improving cement-based materials by using silica fume," *J. Mater. Sci.* 37(4), 673-682.
- Kang, S.T., Lee, B.Y. Kim, J.K. and Kim, Y.Y. (2011), "The effect of fibre distribution characteristics on the flexural strength of steel fibre-reinforced ultra high strength concrete," *Const. Build. Mater.*, **25**(5), 2450-2457.
- Kesner, K. and Billington, S.L. (2005), "Investigation of Infill Panels Made from Engineered Cementitious Composites for Seismic Strengthening and Retrofit," *J. Struct. Eng.*, 131(11), 1712-1720.
- Lee, C.L., Huang, R., Lin W.T. and Weng, T.L. (2012), "Establishment of the durability indices for cement-based composite containing supplementary cementitious materials," *Mater. Des.*, 37, 28-39.
- Lin, W.T. Cheng, A. Huang, R. Chi, M.C. and Hwang, H. (2011), "Properties Evaluation of Cement-based Composites Containing Steel Fiber and Silica Fume," *Adv. Sci. Lett.*, 4(3), 1155-1164.
- Lothenbach, B., Scrivener, K. and Hooton, R.D. (2011), "Supplementary cementitious materials," *Cem. Concr. Res.*, 41(12), 1244-1256.
- Nili, M. and Afroughsabet, V. (2012), "Property assessment of steel-fibre reinforced concrete made with silica fume," *Const. Build. Mater.*, 28, 664-669.
- Sahin, Y. and Koksals, F. (2011), "The influences of matrix and steel fibre tensile strengths on the fracture energy of high-strength concrete," *Const. Build. Mater.*, **25**(4), 1801-1806.
- Swaddiwudhipong, S. Lu, H.R. and Wee, T.H. (2003), "Direct tension test and tensile strain capacity of concrete at early age," *Cem. Concr. Res.*, 33(12), 2077-2084.